Received: 23 February 2021 | Revised: 24 August 2021 | Accepted: 23 September 2021

DOI: 10.1111/fwb.13835

Freshwater Biology WILEY

ORIGINAL ARTICLE

Modelling key variables for understanding the effects of grazing and nutrient recycling by zooplankton on the freshwater microbial loop

Luca Schenone[1] | Beatriz Modenutti[1] | Nicolás Martyniuk[1] | Marcela Bastidas Navarro[1] | Cecilia Laspoumaderes[1,2] | Esteban Balseiro[1]

[1]Laboratorio de Limnología, INIBIOMA, CONICET-Universidad Nacional del Comahue, Bariloche, Argentina

[2]Shelf Sea System Ecology, Alfred-Wegener-Institut, Helmholtz-Zentrum für Polar- und Meeresforschung (AWI), Biologische Anstalt Helgoland, Helgoland, Germany

Correspondence
Esteban Balseiro, Laboratorio de Limnología, INIBIOMA, CONICET-Universidad Nacional del Comahue, Bariloche, Argentina.
Email: ebalseiro@comahue-conicet.gob.ar

Funding information
Fondo para la Investigación Científica y Tecnológica; Consejo Nacional de Investigaciones Científicas y Técnicas

Abstract

1. Pelagic microbial food webs are structured by zooplankton through grazing and nutrient recycling. Cladocerans and copepods are assumed to have different effects on the microbial loop by grazing on different prey sizes and releasing phosphorus (P) differentially. Here, we assessed this effect of differential zooplankton grazing and nutrient recycling on microbial loop dynamics using a combination of experimental and modelling approaches.
2. We performed field incubation experiments in an oligotrophic mountain lake (north-Patagonian Andes) using the natural microbial community and the two dominant zooplankton taxa: a cladoceran (*Diaphanosoma chilense*) and a copepod (*Boeckella gibbosa*). The effect of zooplankton grazing and nutrient recycling were assessed separately in different treatments with direct and indirect zooplankton presence, respectively. We built a mechanistic model to estimate zooplankton grazing and P recycling and prey P quotas. The model was parameterised with the results from our field experiment and with prior information from size-based traits and zooplankton C:P using a Bayesian approach. Laboratory experiments for zooplankton P excretion were also performed to test the predictive accuracy of our model.
3. Our model showed that copepods and cladocerans have contrasting effects on the microbial loop. *Diaphanosoma chilense* grazed mainly on picoplankton while *B. gibbosa* grazed on nanoflagellates and algae. *Diaphanosoma chilense* reduced the biomass and increased P quota of picoplankton, and reduced the P quota of nanoflagellates. In contrast, *B. gibbosa* released more P, increasing the picoplankton biomass and reducing the biomass of nanoflagellates, but increasing its P quota.
4. Based on our experimental and model results, copepod grazing favours higher P acquisition rates for cladocerans by releasing more P for picoplankton. By contrast, cladocerans would have a mixed effect on the main food items of copepods by increasing P quotas of the strict osmotrophic algae but decreasing P quotas of nanoflagellates.
5. Our mechanistic model is useful to quantitatively assess key planktonic variables, which are usually difficult to measure in the field, such as zooplankton P excretion

rates and microbial P quotas, by using more conspicuous variables such as biomass of the different microbial compartments and dissolved and particulate P concentrations.
6. The model presented here could be used to disentangle complex pathways in the microbial food web. The relative importance of phagotrophy and osmotrophy in P uptake, P quotas, and nutrient recycling by grazers result in key variables for understanding ecosystem matter flux and resource use efficiency.

KEYWORDS
bacterivory, Bayesian approach, ecological stoichiometry, mixotrophic nanoflagellates, phosphorus quota

1 | INTRODUCTION

The dynamic of the pelagic microbial food web has important implications for ecosystem biogeochemical fluxes and energy transfer (Cotner & Biddanda, 2002). This microbial food web, referred to as the *microbial loop* (Azam et al., 1983) includes multiple compartments such as heterotrophic bacteria, autotrophic picoplankton, nanoflagellates (mixotrophic and heterotrophic), and ciliates. Planktonic protists, nanoflagellates and ciliates, consume bacteria, and, in turn, serve directly as major prey items for most zooplankters. However, this simplified scheme results in complex top-down and bottom-up relationships, due to grazing and nutrient recycling (Vanni, 2002).

Together with direct consumption of prey, nutrient recycling is now recognised as an essential link between predators and lower trophic levels (Schmitz et al., 2010). Empirical evidence from the last 3 decades highlights the importance of consumers in biogeochemical cycles (Atkinson et al., 2017; Attayde & Hansson, 1999; Sitters et al., 2017; Vanni, 2002). The incorporation of nutrient recycling in food web models pointed out the importance of size-based physiological traits, such as nutrient affinity and internal store ability (Edwards et al., 2012). This aspect also becomes relevant in the study of the eco-evolutionary dynamics of predators and their prey (Branco et al., 2020). In current food web modelling, there is a growing interest among ecologists to integrate both empirical and theoretical approaches to understand the role of predators in nutrient cycling (Atkinson et al., 2017).

In planktonic food webs, zooplankton act as a sink for nutrients by incorporation into biomass through predation, and as a source by releasing dissolved nutrients (Branco et al., 2018; Elser & Urabe, 1999). The elemental composition of zooplankton is usually more homeostatic than their prey, and zooplankton, therefore, recycle surplus nutrients back into the environment when faced with nutritionally imbalanced food (Sterner & Elser, 2002). Zooplankton-mediated nutrient recycling may change the availability of essential nutrients such as phosphorus (P) and nitrogen (N; Elser & Urabe, 1999). The recycling rate of a particular element will depend on the elemental requirements of the dominant zooplankton (Balseiro et al., 1997; Elser et al., 1988). In particular, copepods tend to have a relatively higher body C:P than cladocerans and thus recycle more P (Elser et al., 1988; Sterner & Elser, 2002). Therefore, planktonic communities dominated by contrasting zooplankton groups may intensify or mitigate nutrient limitation of their prey by being an effective sink or source of specific elements (Balseiro et al., 1997; Branco et al., 2018; Hessen et al., 1992).

Microbial food webs are directly linked to higher trophic levels through zooplankton grazing (Jürgens, 1994; Li et al., 2014). Within the microcrustacea, cladocerans and copepods produce differential grazing impact on microbial compartments (Modenutti et al., 2003; Zöllner et al., 2003). Pelagic cladocerans can access almost all compartments of the microbial loop since they can effectively filter a wide range of particle sizes (Brendelberger, 1991). Early studies have reported that different *Daphnia* species can access small particles such as bacteria (Gophen & Geller, 1984; Jürgens, 1994), while other studies have demonstrated the higher efficiency of the sidid *Diaphanosoma* as a bacteria feeder (Brendelberger, 1991; Gophen & Geller, 1984). Despite this high efficiency, *Diaphanosoma* was seldom considered as a direct bacteria grazer, so their potential competitive effect on other bacterivores (such as nanoflagellates) was ignored. By contrast, copepods are not important bacterial grazers (Sanders et al., 1989) but can effectively consume nanoflagellates and ciliates (Vrede & Vrede, 2005). Boeckellids in particular are the dominant calanoid copepods of the Southern Hemisphere, and reported as consumers of mixotrophic protists (Balseiro et al., 2001; Burns & Schallenberg, 1996; Modenutti et al., 2003). Therefore, zooplankton appear to play an important role in structuring microbial food webs by grazing different prey compartments. Currently, modelling the combined effect of zooplankton feeding strategies and nutrient excretion on the microbial food web represents a challenge in ecology (Branco et al., 2018; Lignell et al., 2013; Ptacnik et al., 2004).

In environments where P is the limiting nutrient, as in many freshwater oligotrophic lakes, planktonic microbial communities (bacteria, autotrophic picoplankton, protists) account for most of the primary production and energy transfer to higher trophic levels (Cotner & Biddanda, 2002). The affinity for dissolved P is higher for small-sized picoplankton than larger phytoplankton due to the higher surface/volume ratio, allowing picoplankton to attain higher P concentration

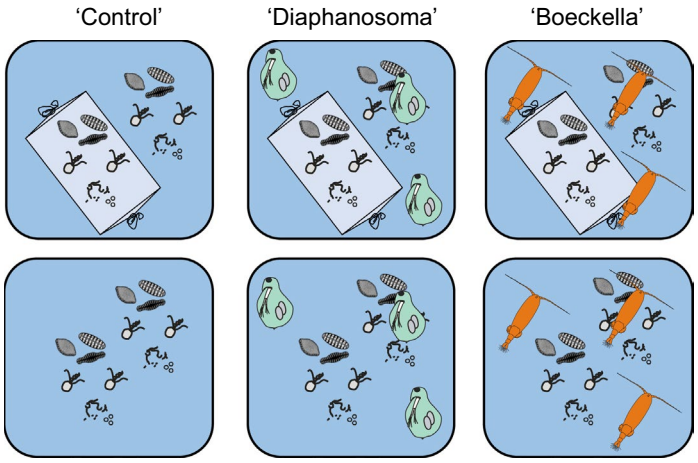

FIGURE 1 Design of the experiment performed in lake Los Cántaros. The experiment consisted of a factorial design with six treatments. R treatments were performed using dialysis bags to avoid zooplankton grazing, thus only the nutrient recycling effect was present inside the bags. R + G treatments were performed without the dialysis bags allowing direct contact of the zooplankton with the lower trophic levels, thus both grazing and nutrient recycling effects were present

per unit of biovolume (hereafter P quota) than larger cells (Branco et al., 2020; Edwards et al., 2012; Tambi et al., 2009). Moreover, the combination of autotrophic and heterotrophic modes of nutrition represents an advantage for mixotrophic algae (e.g. nanoflagellates) by feeding on P-rich picoplankton (Yvon-Durocher et al., 2017). As a consequence, zooplankton grazing differentially on prey with different P quotas would result in differences in P acquisition and excretion rates (Elser et al., 1996; Laspoumaderes et al., 2015).

Accurate parameterisation of food web models is a challenge since they rapidly increase in complexity when several prey and predator levels are involved (Anderson, 2005; Loreau & De Mazancourt, 2013). Fortunately, the Bayesian approach appears to be an alternative to the classical methods that rely on the likelihood function (Arhonditsis et al., 2008; Clark, 2005; Zhang & Arhonditsis, 2009). Bayesian methods were successfully applied to estimate key planktonic traits based on cell sizes, such as nutrient affinity and ingestion rates quantified from mesocosm experiments that focused on the microbial loop (Lignell et al., 2013). A similar approach, using prior information from the literature, succeeded in identifying the role of total N and P concentrations and zooplankton in governing algal mass occurrence during an 8-year monitoring study in a Finnish lake (Malve et al., 2007). In the present work, we modelled the effect of zooplankton grazing and P recycling on the abundance and P quota dynamics of the microbial loop. To achieve this, we combined two different approaches: (1) field experiments in an oligotrophic lake where zooplankton grazing and nutrient recycling effects were assessed separately; and (2) a mechanistic model that was parameterised with the results of the field experiments and prior information using a Bayesian approach. For our field experiments, we chose two contrasting zooplankton taxa: a copepod (*Boeckella gibbosa*) and a cladoceran (*Diaphanosoma chilense*). We expected that the biomass and P quota of the lower trophic levels (bacteria, autotrophic picoplankton, mixotrophic nanoflagellates, and algae) would be affected by the differential grazing and P recycling of these two zooplankton species. Finally, with our model, we aimed to predict particulate and dissolved P dynamics within the planktonic food web, which has important implications for production studies in oligotrophic systems.

2 | METHODS

2.1 | Study site and planktonic community

The experimental study was carried out in the glacial lake Los Cántaros (north-western Patagonia, Argentina, 41°00′S, 71°49′W) located at 1,000 m above sea level in the Andes mountain range, 3 km from the Puerto Blest Biological Station (Universidad Nacional del Comahue). The lake has 14 m of maximum depth and is oligotrophic (chlorophyll $a < 1$ μg/L), transparent (>1% of photosynthetically active radiation [PAR, 400–700 nm] penetrates to maximum depth), with strong P limitation (Souza et al., 2010; Villar-Argaiz et al., 2018). North Andean patagonian lakes have very dilute waters, with ion concentrations below world average (Markert et al., 1997). Lake Cantaros in particular has a very low conductivity (<40 μS/cm). The phytoplankton is mostly dominated by picoplanktonic cyanobacteria (Pcy) and small mixotrophic nanoflagellates such as the haptophyte *Chrysochromulina parva* (Carrillo et al., 2017; Schenone et al., 2020). Larger phytoplankton species are less abundant and are represented mainly by small diatoms (*Cyclotella* spp.) and autotrophic dinoflagellates (*Gymnodinium paradoxum*). The crustacean zooplankton is dominated by two species, the calanoid copepod *Boeckella gibbosa*, and the cladoceran *Diaphanosoma chilense*.

2.2 | Field incubation experiments

We determined the effect of grazing (G) and nutrient recycling (R) of the copepod *B. gibbosa* and the cladoceran *D. chilense* with a short-term incubation experiment (48 hr) carried out at midsummer (4–6 February 2020). Experimental units consisted of transparent polystyrene 1-L flasks filled with natural lake water gently filtered through a 55-μm mesh net to remove zooplankton. Experimental units were divided according to the different treatments and incubation time with four replicates each. The experiment consisted of a factorial design with six treatments: R Control, R *Diaphanosoma*, R *Boeckella*, R + G Control, R + G *Diaphanosoma* and R + G *Boeckella* (Figure 1). R + G Treatments (both G and R effects present) consisted

of flasks (experimental units) with direct zooplankton presence (five individuals of *B. gibbosa* or *D. chilense*) or without zooplankton (R + G Control). R treatments consisted of an indirect zooplankton presence (only R effect present) and this condition was achieved using two dialysis bags inside the experimental units (Sigma™, USA; 12,000–14,000 Da pore-size, *c*. 8 cm flat width, cut to a length of 15 cm *c*. 300 ml capacity). The bags were washed with distilled water for 3 hr and left overnight in MilliQ water. Before the field experiments, we checked in the laboratory that the pre-washed dialysis bags did not release any dissolved nutrients (dissolved organic carbon [DOC], total dissolved nitrogen [TDN], or total dissolved phosphorus [TDP]) to the water. The bags were transported to the field in MilliQ water. Dialysis bags of 300 ml were placed inside the 1-L flasks and filled with the filtered lake water. Then, five zooplankton individuals (*B. gibbosa* or *D. chilense*) were placed inside the flask in the R + G treatments or inside the flaks but outside the dialysis bags in the R treatments (Figure 1). In our experiment, we used *B. gibbosa* CV instar (*c*. 1.6 mm) or adults of *Diaphanosoma chilense* (*c*. 1.5 mm). Finally, R control treatments consisted of the same procedure using 1-L flasks with the dialysis bags and no zooplankton addition. All the experimental units were submerged in the lake at 2 m depth (58% of surface PAR) and four replicates of each treatment were removed after 24 and 48 hr.

After removal from the water, experimental units were carried immediately to the laboratory at the Puerto Blest Biological Station, in darkness in thermally insulated containers. The water inside the 1-L flasks (R + G) or inside the dialysis bags (R) was collected for the different analyses as follows. A volume of 150 ml was used to analyse total phosphorus (TP) and TDP. A volume of 60 ml was preserved with buffered formaldehyde (final concentration, 2% v/v) for bacteria, autotrophic picoplankton and nanoflagellate counting. These samples were stored refrigerated in darkness and quantified within 2 weeks of sampling. Finally, a volume of 50 ml was preserved with acid Lugol solution for algae and ciliate quantification.

2.3 | Field nanoflagellate bacterivory experiments

Nanoflagellate bacterivory was estimated using fluorescently labelled bacteria (FLB). The FLB were prepared following Šimek and Chrzanowski (1992). After prefiltration through a 2-μm pore filter, we concentrated the bacterioplankton in a 0.22-μm pore filter (Nucleopore). Cells were detached from the filter surface by sonication, and were heat-killed and stained with 5-([4,6-ichlorotriazin-2-yl] amino) fluorescein (DTAF) according to Sherr et al. (1987). FLB were stored in 2 ml aliquots at −20°C. The obtained FLB were measured and counted under an epifluorescence microscope to verify shape, size, and abundance. The obtained FLB were mostly coccoid shaped of 0.76 ± 0.21 μm in diameter.

Experiments were carried out in 150-ml ground-stoppered glass bottles, with three replicates per time interval. The bottles were filled with lake water filtered through a 55-μm mesh net to remove zooplankton. FLB were then added to each bottle at a final concentration of 20% of total bacterial abundance. The bottles were submerged in the lake at 2 m depth (58% of surface PAR). At different time intervals (5, 10, 15, 20, and 40 min), three replicates were removed and fixed in situ with 0.5% of Lugol solution, followed by 2% formaldehyde and drops of 3% sodium thiosulphate to clear the colour (Kemp et al., 1993).

2.4 | Laboratory experiments

We measured the P excretion and egestion of *B. gibbosa* and *D. chilense* following Laspoumaderes et al. (2015). Zooplankton samples were collected with a plankton net (200-μm mesh) by making at least three independent horizontal tows in the central pelagic area of the lake. Individuals of both species were carefully transported in natural lake water (filtered through 55-μm mesh) to the Puerto Blest Biological Station. We placed 10 individuals of *B. gibbosa* or 10 of *D. chilense* in 125-ml beakers (six replicates per each species) filled with Milli-Q water. Due to the extremely low conductivity of Lake Los Cantaros (<40 μS/cm), *D. chilense* and *B. gibossa* did not show any sign of stress (swimming, body integrity, and/or swelling). However, these excretion data were not used in the model calibration, but only to compare with the model output. After 4 hr, the crustaceans were gently removed with a clean pipette and the water was filtered through acid-washed and pre-combusted (450°C, 2 hr) GF/F Whatman filters. The filters were analysed for total particulate phosphorus and the filtered water for TDP. Finally, the zooplankton individuals were collected and designated for body C and P content analyses.

2.5 | Laboratory determinations

Total phosphorus was determined using unfiltered lake water and TDP was determined using lake water filtered through GF/F filters. Samples for P determination (TDP and TP) were digested with potassium persulphate at 125°C at 1.5 atm for 1 hr. Then, P concentrations were determined with the ascorbate-reduced molybdenum method (APHA, 2005) and absorbance measured in 100 mm cuvettes with a Shimadzu UV2450 dual-beam spectrophotometer (Detection limits: 0.5 μg/L = 0.016 μmol/L).

Total particulate phosphorus from the laboratory excretion experiment was determined on the precombusted and acid-washed GF/F filters. Filters were placed in 45 ml MilliQ water. P content of cladoceran and copepods were obtained placing 10 individuals of each species (previously rinsed in MilliQ water) in 45 ml MilliQ water. In both cases, P concentration was determined as TP.

Zooplankton body C content was obtained by placing individuals separately onto pre-combusted (2 hr at 450°C) GF/F Whatman filters and analysed in a Thermo Finnigan EA 1112 CN elemental analyser (Thermo Scientific).

For bacteria quantification, 3 ml from the field experiment samples were stained with fluorochrome 4′, 6-diamidino-2-phenylindole

(DAPI; final concentration 0.2% w/v) according to Porter and Feig (1980). Counting was done on black membrane filters (Poretics, 0.2 μm pore size) at 1,250× magnification in an Olympus BX50 epifluorescence microscope (Olympus) using UV light (U-MWU filter). Picocyanobacteria were counted on black polycarbonate filters (Poretics, 0.2 μm pore size) by autofluorescence using the same microscope fitted with blue light (U-MWB filter, Excitation 450–480 nm, Emitter 515 Long Pass, Beam Splitter 500 nm) and green light (U-MWG filter, Excitation: 510–550 nm, Emitter: 590 Long Pass Beam Splitter 570 nm). Finally, a volume of 40 ml was stained with DAPI (final concentration 0.2% w/v) and filtered onto - μm black membrane filters (Poretics) for the enumeration of nanoflagellates. Cells were counted by epifluorescence microscopy at 1,250× magnification, using both UV and blue and green light (filters as above), to distinguish between heterotrophic nanoflagellates and mixotrophic nanoflagellates. Phytoplankton quantification was performed using an inverted microscope and Utermöhl chambers. An image analyser was used for counting and size measurements (Image Pro Plus, Media Cybernetic). At least 30 cells of each pico- and phytoplankton species were measured and cell biovolume was calculated by approximation to appropriate geometric figures (Sun & Liu, 2003).

Finally, samples from the nanoflagellate bacterivory experiments were stained with DAPI and filtered through 1-μm pore size black polycarbonate filters. The number of ingested FLB per flagellate was assessed with the same epifluorescence microscope by alternating between UV light and blue light. At least 100 flagellates were checked on each filter. Each experimental treatment was run in three replicates and at least three filters were prepared for each replicate. Uptake rates were estimated by the linear regression between time and number of bacteria ingested per cell which was calculated based on the number of FLB and the FLB:bacteria ratio in each replicate (Sherr, 1993). The obtained uptake rates were converted into biomass of prey (mm^3) ingested per biomass of nanoflagellates (mm^3) per day and these data were supplied as prior information for the bacterivory parameters of our mechanistic model.

2.6 | Model description

We developed a mathematical model to represent how contrasting predators change biomass and P quota of their prey through grazing and nutrient recycling. The model was built based on the composition of the natural plankton community of Lake Los Cántaros and our understanding of the trophic relationships within this P-limited environment (Carrillo et al., 2017; Souza et al., 2010; Villar-Argaiz et al., 2018). In our studied system we identified five microbial compartments (i), and two zooplankton components (j). Microbial compartments were (i = 1): heterotrophic bacteria <1 μm in maximum length; (i = 2): Pcy <1.5 μm; (i = 3) nanoflagellates 2–10 μm (mainly mixotrophic nanoflagellates *C. parva* and *Pseudopedinella* sp.); (i = 4) algae 8–35 μm (mainly *Cyclotella* spp. and *G. paradoxum*), and (i = 5) Pcy colonies (CPcy) corresponded to aggregates of 10–12 cells in average reaching 14–15 μm in diameter. The two zooplankton compartments were the copepod *B. gibbosa* (j = 1) and the cladoceran *D. chilensis* (j = 2). A list of all variables and parameter with their respective units can be found in Table S1 of the Supplementary Information.

Dissolved P (P) dynamics during the experimental time (t) was fitted with a differential equation:

$$\frac{dP}{dt} = \sum_{i=1}^{5} X_i(-V_i + Q_i * m_i) + \sum_{j=1}^{2} R_j Z_j \quad (1)$$

where X_i is the biomass of the ith prey compartment, V_i corresponds to P uptake by the ith prey compartment, Q_i is the P quota of the ith compartment, m_i is the mortality rate of ith compartment, thus, $Q_i * m_i$ corresponds to P recycling due to prey death, R_j is the total excretion by jth zooplankton, and Z_j is the abundance of jth zooplankton.

Prey P uptake (V_i) was modelled as a function of P following Michaelis–Menten uptake kinetics:

$$V_i = f_{max_i}\left(\frac{P}{k_i + P}\right) + \sum_{n=1}^{2} b_{max_n}\left(\frac{B_n Q_n}{k'_n + B_n Q_n}\right) \quad (2)$$

where f_{max_i} is the maximum nutrient uptake rate of the ith prey compartment and k_i is the half saturation constant. A second Michaelis–Menten term $\sum_{n=1}^{2} b_{max_n}\left(\frac{B_n Q_n}{k'_n + B_n Q_n}\right)$ was added to the equation above to account for nanoflagellate P uptake through bacterivory (B_n). Therefore, this term equals zero in the strict osmotrophic compartments (heterotrophic bacteria, Pcy, micro-algae and CPcy).

Furthermore, we modelled prey dynamics (X_i) using the same approach as with P. We fit a differential equation for prey dynamics during the experimental time:

$$\frac{dX_i}{dt} = X_i(u_i - m_i) - B_i X_3 - \sum_{j=1}^{2} G_{i,j} Z_j \quad (3)$$

where X_i increases according to their growth rate (u_i) and decreases according to their mortality rate (m_i) and their grazing by zooplankton j ($G_{i,j}$). In the case of heterotrophic bacteria (X_1) and Pcy (X_2) dynamics, we added a bacterivory term (B_i) exerted by nanoflagellates (X_3).

Prey growth rate (u_j) was modelled as a function of their cellular P quota using Droop's formulation (Droop, 1968):

$$u_i = \mu_{max_i}\left(1 - \frac{Q_{min_i}}{Q_i}\right) \quad (4)$$

where parameter μ_{max_i} is the maximum growth rate of ith prey and parameter Q_{min_i} is the lower bound of ith prey P quota (Q_i).

Prey P quota (Q_i) increases due to P uptake and declines due to dilution by growth according to Droop's formulation (Droop, 1973):

$$\frac{dQ_i}{dt} = V_i - u_i * Q_i \quad (5)$$

Zooplankton grazing ($G_{i,j}$) on each of the five prey compartments, as well as nanoflagellate bacterivory (B_i) on bacteria and Pcy prey,

were modelled using the classical Holling's type II functional response (Holling, 1959):

$$G_{i,j} = \frac{a_{i,j} X_i}{1 + a_{i,j} h_{i,j} X_i} \quad (6)$$

$$B_i = \frac{a'_i X_i}{1 + a'_i h'_i X_i} \quad (7)$$

where parameters $a_{i,j}$ correspond to the attack rate and $h_{i,j}$ is the handling time of zooplankton species j. Parameters a'_i and h'_i correspond to the attack rate and handling time of nanoflagellates (X_3).

Particularly, for Pcy single-cells and colonies (CPcy) we considered two extra terms of aggregation of Pcy single-cells in response to predation by nanoflagellates and cladocerans (Callieri, 2010). These terms were negative for Pcy (X_2) and positive for CPcy (X_5) according to a decrease and increase in biomass, respectively:

$$\frac{dX_2}{dt} = X_2(u_2 - m_2) - B_2 X_3 - B_2 X_3 ag_{NF} - G_{2,2} Z_2 ag_{Cl} - G_{2,2} Z_2 \quad (8)$$

$$\frac{dX_5}{dt} = X_5 (u_5 - m_5) + B_2 X_3 ag_{NF} + G_{2,2} Z_2 ag_{Cl} - G_{5,1} Z_1 \quad (9)$$

where parameters ag_{NF} and ag_{Cl} are coefficients for the proportion of aggregated Pcy under grazing pressure by nanoflagellates ($B_2 X_3$) and the cladoceran *D. chilense* ($G_{2,2} Z_2$).

Finally, zooplankton P recycling (R_j) was modelled as a function of their body C:P ratio (CP_j), their grazing rates ($G_{i,j}$) and P quota of their prey (Q_i):

$$R_j = r_j CP_j \sum_{i=1}^{5} G_{i,j} Q_i \quad (10)$$

where $\sum_{i=1}^{5} G_{i,j} Q_i$ represents P acquisition of zooplankton j and parameter r_j is a conversion factor for the body C:P ratio. Therefore, $r_j CP_j$ represents the proportion of phosphorus that is not extracted from the ingested prey and is released by zooplankton j (Branco et al., 2020; Elser et al., 1996; Grover, 2004).

2.7 | Model calibration

We fit our model equations with data from the field experiments using Bayesian Markov chain Monte Carlo (MCMC). The MCMC technique utilises consecutive model simulations with judicious parameter updating to produce a sample from the prior probability distributions chosen for the model parameters (Haario et al., 2006). Within this Bayesian framework, all the unknown quantities are described by their statistical probability distributions, whether they are model parameters, unknown states of the system in question, or model predictions (Haario et al., 2006; Malve et al., 2007). To fit the differential equations from our model to the experimental data, we performed a discretisation following the formulation

$$A_{t+dt} = A_t dt \frac{dA}{dt} \quad (11)$$

where A_t correspond to each of our dynamic compartments (P, X_i, and Q) at time step t and is updated to the next time step $t + dt$ by multiplying the actual state by its derivate.

Priors for initial dynamic parameter values were applied, assuming positive half-normal probability distributions (Table S1). Particularly, we choose highly informative priors for prey traits parameters (mortality and growth rates, P affinity and bacterivory rates). Mortality rates for all prey compartments were fixed to 0.1 day^{-1} according to Branco et al. (2020). Priors for μ_{max}, f_{max}, k, and Q_{min} were obtained from known allometric relationships with cellular size in freshwater phytoplankton (Edwards et al., 2012) and protists and bacteria (Tambi et al., 2009). Priors for bacterivory parameters b_{max} and hr were obtained from the results of the bacterivory experiments. Likewise, priors for the body C:P ratios of zooplankton (CP) were obtained from our own measurement of particulate C and P. On the contrary, we choose non-informative priors for zooplankton attack rates (a) and conversion factor for P recycling (r) assuming half normal distributions of mean $\mu = 0$ and variance $\tau = 1$, thus, posterior values for these parameters were estimated only from our experimental data without previous assumptions. A sample of possible parameter values was obtained with the MCMC algorithm, forming the posterior distribution of the parameter. We checked parameter convergence using five MCMC chains with 2×10^5 iterations each and a burn-in phase of 1×10^5 iterations. Finally, we used parameter posteriors from the model equation to simulate P recycling rates of cladoceran and copepods and prey P quota at $t = 72$ hr. Bayesian analysis and predictions were performed using JAGS (Plummer, 2003) interfaced through R Studio (R Team, 2020).

2.8 | Statistical analysis

From our field experiment results, we performed two-way ANOVA to compare biomass of the prey compartments and dissolved and particulate P concentrations between the treatments (factor with six levels: R Control, R *Diaphanosoma*, R *Boeckella*, R + G Control, R + G *Diaphanosoma* and R + G *Boeckella*) and incubation time (factor with two levels: 24 and 48 hr). When the p-value from the ANOVA was significant, we performed a posteriori Dunnett's tests to determine differences between zooplankton treatments and the control treatments. Finally, to assess zooplankton effect on the quantities estimated by our model (i.e. prey P quotas and zooplankton P recycling rates), we estimated the difference between the posterior distributions of the zooplankton treatments and the control treatments and calculated the proportion of posterior values with the same sign as the mean using JAGS (Plummer, 2003).

3 | RESULTS

3.1 | Field incubation experiments

We found a statistically significant difference in the biomass (mm^3/L) of the different prey compartments between treatments (two-way ANOVA, $p < 0.05$ for all compartments except CPcy, Table S2) and incubation time (two-way ANOVA, $p < 0.01$ for all compartments, Table S2), although the interaction between these terms was not significant. Since no differences between the control R and the control R + G treatments were found at 24 and 48 hr of incubation, they were pooled as *control* for a posteriori comparison with zooplankton treatments. Differences between zooplankton treatments and the control were observed at 48 hr of incubation (Figure 2 lower panel). In the grazing treatments (R + G), the biomass of nanoflagellates and algae were lower in the presence of the copepod *B. gibbosa* (a posteriori Dunnett's test $p = 0.004$ and $p = 0.023$, respectively). The presence of the cladoceran *D. chilense* resulted in lower biomass of heterotrophic bacteria and Pcy (a posteriori Dunnett's test $p = 0.009$ and $p = 0.013$, respectively), higher biomass of CPcy (a posteriori Dunnett's test $p = 0.023$) and marginally lower biomass of nanoflagellates (a posteriori Dunnett's test $p = 0.088$). Regarding the nutrient recycling treatments (R), the only significant effect for the indirect presence of *B. gibbosa* was for CPcy (a posteriori Dunnett's test $p = 0.021$). Similarly, no significant differences in prey abundance were observed between the indirect presence of the cladoceran *D. chilense* and the control. Futhermore, similar patterns were observed at 24 hr of incubation, that is, no significant differences between the zooplankton treatments and the control were detected (Figure 2 upper panel).

During the experiments, the colony size of CPcy (cells/colony) increased after 48 hr of incubation related to *D. chilense* predation (Figure 3). Colony size was different between treatments (two-way ANOVA, $p < 0.001$, Table S2) and incubation time (two-way ANOVA, $p = 0.002$, Table S2), and the interaction between these two terms was significant (two-way ANOVA, $p = 0.016$, Table S2). Compared to the control with no zooplankton, the number of cells per colony was higher in the R + G treatment with direct presence of *D. chilense* (a posteriori Dunnett's test $p = 0.008$). In addition, we observed a statistically marginal decrease in the number of cells per colony in

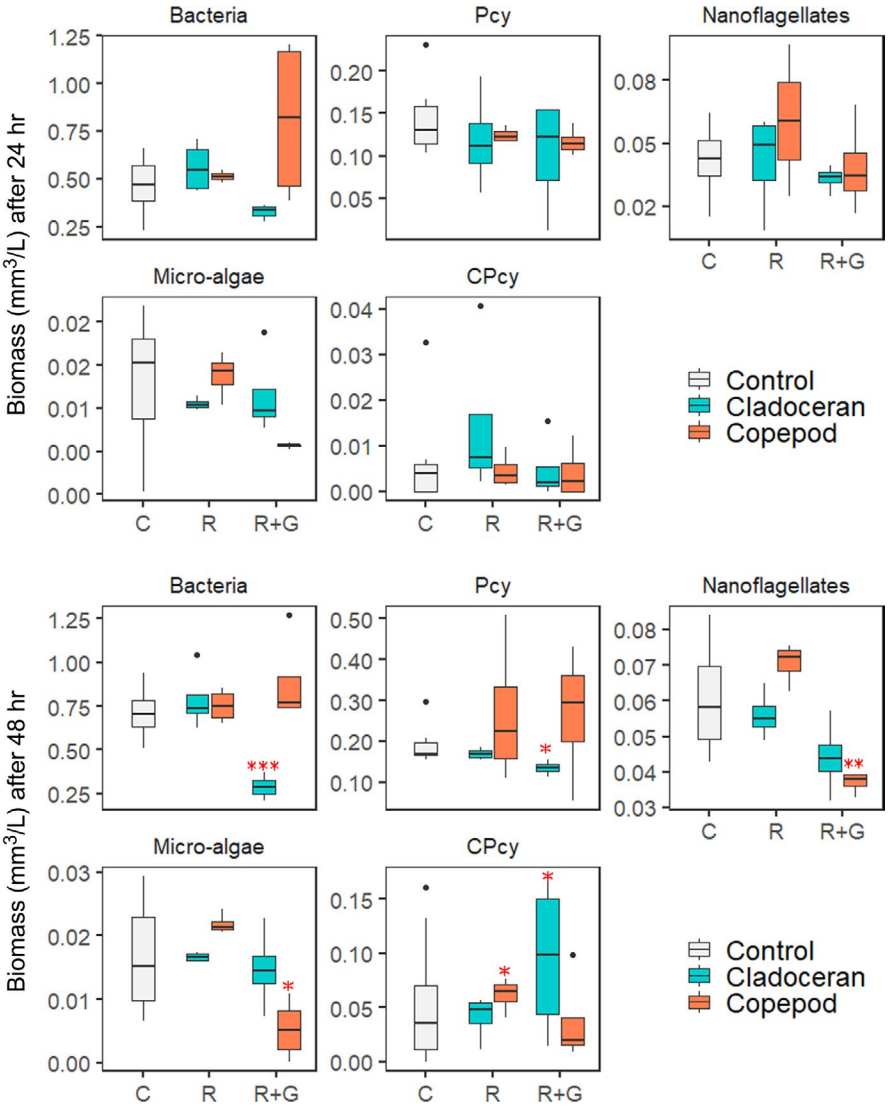

FIGURE 2 Biomass after 24- and 48-hr incubation of the five prey compartments under the direct and indirect presence of the cladoceran *Diaphanosoma chilense* and the copepod *Boeckella gibbosa*. C = control treatments with no zooplankton (R and R + G pooled together); R = recycling treatments with zooplankton and prey separated by dialysis bags; R + G = grazing treatment with direct contact between zooplankton and prey. Black dots correspond to outliers and red asterisks represent significant differences of the zooplankton treatments with the control (*$p < 0.05$, **$p < 0.01$, ***$p < 0.001$)

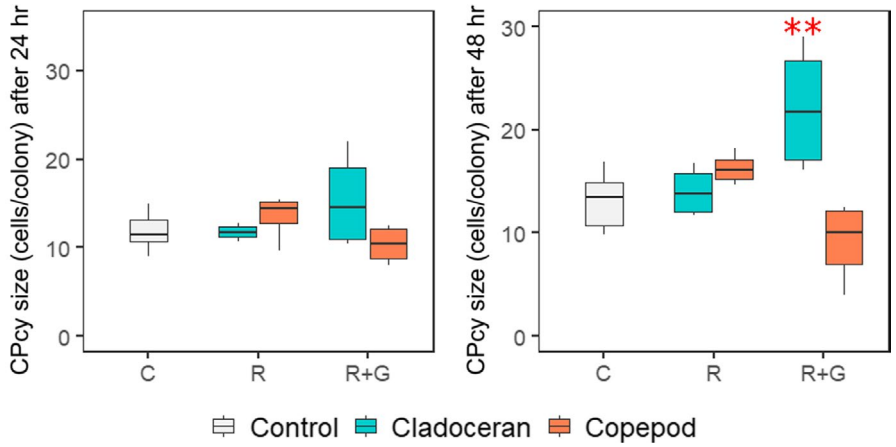

FIGURE 3 Picoplanktonic cyanobacteria colony (CPcy) sizes under the direct and indirect presence of the cladoceran *Diaphanosoma chilense* and the copepod *Boeckella gibbosa*. C = control treatments with no zooplankton (R and R + G pooled together); R = recycling treatments with zooplankton and prey separated by dialysis bags; R + G = grazing treatment with direct contact between zooplankton and prey. Black dots correspond to outliers and red asterisks represent significant differences of the zooplankton treatments with the control (*$p < 0.05$, **$p < 0.01$, ***$p < 0.001$)

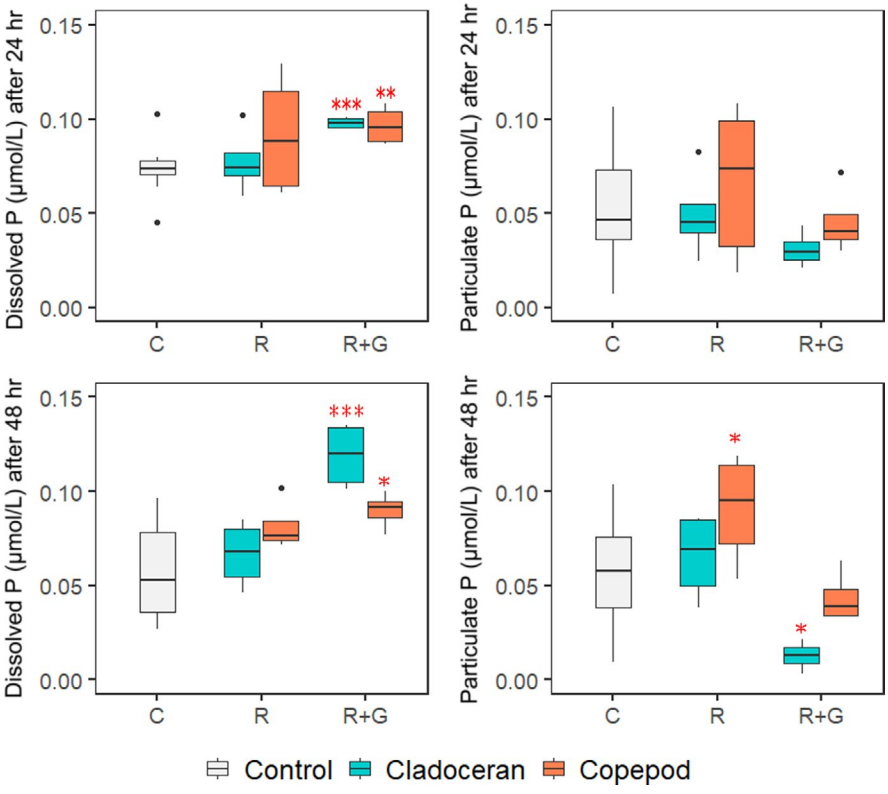

FIGURE 4 Dissolved and particulate phosphorus concentration after 24- and 48-hr incubation under the direct and indirect presence of the cladoceran *Diaphanosoma chilense* and the copepod *Boeckella gibbosa*. C = control treatments with no zooplankton (R and R + G pooled together); R = recycling treatment with zooplankton and prey separated by dialysis bags; R + G = grazing treatment with direct contact between zooplankton and prey. Black dots correspond to outliers and red asterisks represent significant differences of the zooplankton treatments with the control (*$p < 0.05$, **$p < 0.01$, ***$p < 0.001$)

the R + G treatment with direct presence of *B. gibbosa* (a posteriori Dunnett's test $p = 0.077$).

The concentration of dissolved and particulate P (µmol/L) differed among treatments (two-way ANOVA, $p < 0.001$, Table S2) and the interaction between treatments and incubation time was significant only for dissolved P (two-way ANOVA, $p = 0.033$, Table S2). Since no differences between the control R and the control R + G treatments were found at 24 and 48 hr of incubation, they were pooled as a control for a posteriori comparison with zooplankton treatments. Dissolved P at 48 hr of incubation in the R + G treatments was higher than the control, especially with *D. chilense* (a posteriori Dunnett's test $p < 0.001$ for *D. chilense* and $p = 0.037$ for *B. gibbosa*, Figure 4 lower panel). These increases were also significant at 24 hr of incubation (a posteriori Dunnett's test $p = 0.022$ for *D. chilense* and $p = 0.034$ for *B. gibbosa* at 48 hr, Figure 4 upper panel). By contrast, particulate P at 48 hr of incubation in the R + G treatment with the presence of *D. chilense* was lower than the control (a posteriori Dunnett's test $p = 0.027$) and higher in the R treatment with indirect presence of *B. gibbosa* (a posteriori Dunnett's test $p = 0.049$). Finally, no differences

between the R treatment with indirect presence of *D. chilense* and the control were found for dissolved and particulate P.

3.2 | Field nanoflagellate bacterivory experiments

In the bacterivory experiments, we observed that more than 70% of nanoflagellates ingested FLB. The number of FLB ingested increased with incubation time reaching a maximum of 0.64 ± 0.08 FLB/flagellate at 15 min. The uptake rate was 1.25 ± 0.36 FLB flagellate^{-1} hr^{-1}. Moreover, picoplankton (heterotrophic bacteria and Pcy) abundance in these experiments was $1.07 \times 10^6 \pm 0.49 \times 10^5$ cells/ml, corresponding to a biomass of 0.44 ± 0.12 mm^3/L. By contrast, nanoflagellates abundance was $2.32 \times 10^2 \pm 1.12 \times 10^1$ cells/ml corresponding to a biomass of 0.05 ± 0.004 mm^3/L. We used these values to calculate the uptake rate in terms of the relative biomass (mm^3) of the predator (nanoflagellates) and prey (picoplankton). The uptake rate obtained was 0.73 ± 0.25 day^{-1} (Table S1).

3.3 | The model

Grazing rates in the five prey compartments estimated by the model differed between cladocerans and copepods (Figure 4). *Diaphanosoma chilense* grazing pressure (in terms % of the total biomass reduced per individual) was higher on heterotrophic bacteria and Pcy than nanoflagellates and algae (Figure 5 upper panel, Table S3). Accordingly, *D. chilense* prey size ranged from 0.8 to *c*. 18 μm with a higher contribution of small cells of ≤2 μm (Figure 5 lower panel). Contrastingly, *B. gibbosa* grazing pressure was considerably high for nanoflagellates and micro-algae (Figure 5 upper panel, Table S3). *Boeckella gibbosa* prey size ranged from 5 to *c*. 35 μm with a higher contribution of medium-sized cells from *c*. 9 to *c*. 14 μm (Figure 5 lower panel). The grazing rate on nanoflagellates in particular was higher in copepods than in cladocerans, and a low grazing rate was detected on CPcy by *B. gibbosa* (Figure 5 upper panel, Table S3).

Model estimated bacterivory by nanoflagellates on heterotrophic bacteria and Pcy was 0.966 ± 0.016 and 0.199 ± 0.003 mm^3 prey mm^{-3} flagellate day^{-1}, respectively, which is equivalent to 265.3 ± 5.2 and 24.8 ± 0.4 cell flagellate^{-1} day^{-1}, respectively. Both bacterivory and osmotrophy were considered in our model dynamics for P uptake by nanoflagellates (Equation 2), and we found that nanoflagellates' P uptake was higher through bacterivory than osmotrophy (0.13 ± 0.05 and 0.02 ± 0.01 μmol P mm^{-3} day^{-1}, respectively).

In the model dynamics of CPcy (Equation 9), we considered that colonies can increase by reproduction of cells within colonies and by the aggregation of single cells induced by predation. Thus, in the equation we have three terms of increase, one by reproduction and two as a response to predation (one for nanoflagellates and another for *D. chilense*). We found that both terms for aggregation (nanoflagellates = 0.0027 ± 0.0015 and *D. chilense* = 0.0096 ± 0.0032 mm^3/day) were higher than reproduction of cells within the colonies (0.0019 ± 0.0029 mm^3/day).

Prey P quota (Q, nmol/mm^3) estimated by the model showed differences between zooplankton treatments and the control at 48 hr (Figure 6 upper panel). Estimated Q for all the strict osmotrophic prey compartments (heterotrophic bacteria, Pcy, micro-algae, and CPcy) were higher in the R + G treatments of both zooplankton taxa (99.9% of their posterior probability higher than the control treatments, Table S4). By contrast, estimated Q for mixotrophic nanoflagellates was higher under the direct presence of *B. gibbosa* (91.3% of their posterior probability higher than the control treatments, Table S4), but lower under the direct presence of *D. chilense* (78.9% of their posterior probability lower than the control treatments, Table S4). In addition, we performed model predictions for P quota at 72 hr of incubation from the final prey biomass and dissolved P conditions of our field experiments at 48 hr. We found similar patterns to those observed at 48 hr but more pronounced. Particularly, the *B. gibbosa* R treatment showed less variation and higher differences from the control in the case of micro-algae (81.3% of their posterior probability higher than the control treatments, Table S4) and CPcy (82.4% of their posterior probability higher than the control treatments, Table S4). Finally, greater differences in the predicted prey P quotas at 72 hr were found between copepods and cladocerans in the R + G treatments (Figure 6 lower panel).

Model estimated P acquisition rates ($\sum_{i=1}^{5} G_{i,j} Q_i$ from Equation 10), as occurred in grazing rates, were different between copepods and cladocerans. P acquisition rate was higher for *D. chilense* than *B. gibbosa* (2.21 ± 0.16 and 1.29 ± 0.11 nmol P/day, respectively). For the copepod *B. gibbosa*, P acquisition rates by grazing on CPcy, micro-algae and nanoflagellates were 0.03 ± 0.01, 0.82 ± 0.09, and 0.47 ± 0.06 nmol P/day, respectively, representing 2%, 62%, and 36% of their P acquisition. For the cladoceran *D. chilense*, P acquisition rates by grazing on heterotrophic bacteria, Pcy, nanoflagellates and micro-algae were 1.28 ± 0.12, 0.36 ± 0.04, 0.30 ± 0.07, and 0.27 ± 0.03 nmol P/day, respectively, representing 58%, 16%, 14%, and 12% of their P acquisition.

3.4 | Laboratory experiments and model predictions of excretion rates

We obtained body C and P contents of copepods and cladocerans from our laboratory experiments, and C:P molar ratios were 237.25 ± 26.50 for *B. gibbosa* and 73.85 ± 13.77 for *D. chilense*. These values were supplied to our model as prior information for the parameter *CP* to estimate the proportion of P released by zooplankton together with the conversion factor r ($r_j CP_j$ from Equation 10). Posterior values for the parameter r were very similar between copepods and cladocerans (>99.9% overlap between their posterior probabilities, Table S3).

The predictive value of our model was tested by comparing model estimations of P excretion rates with results from the independent excretion laboratory experiments. P excretion rates

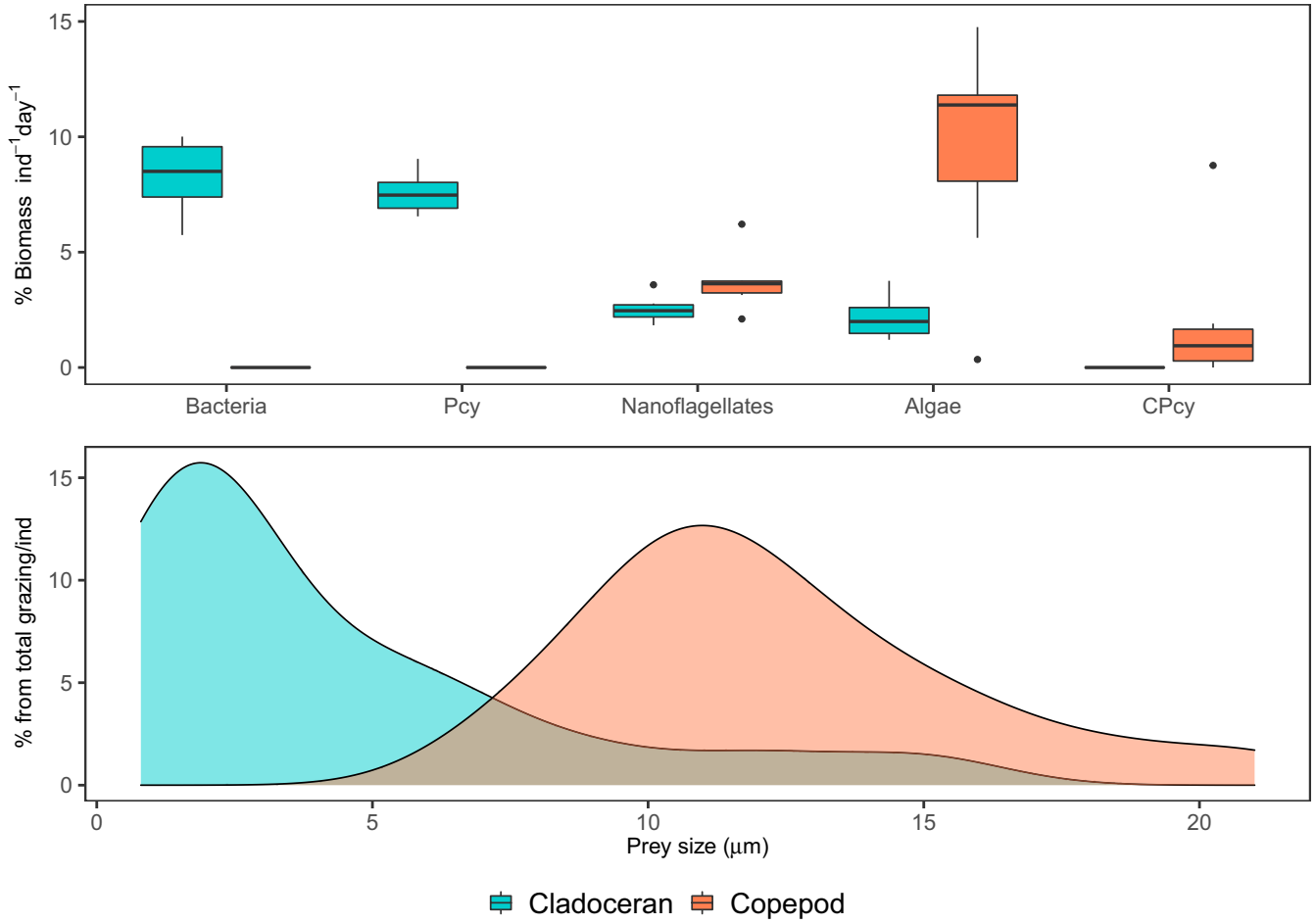

FIGURE 5 Model-estimated grazing rates on the different prey compartments by the cladoceran *Diaphanosoma chilense* (blue) and the copepod *Boeckella gibbosa* (red). Top panel shows zooplankton per capita grazing as % consumed from total prey biomass and bottom panel shows the size (diameter) range of consumed prey. Black dots correspond to outliers

obtained experimentally indicated that copepods release more P (1.71 times) than cladocerans (Figure 7 white boxes). Although these experimental data were not used for model calibration, the model predicted similar results. Noticeably, P excretion rates estimated by our model (Equation 10) showed the same pattern: copepods excreted 1.65 times more P than cladocerans (Figure 7 grey boxes).

3.5 | Conceptual synthesis

Our experimental results and the mechanistic model developed pointed out that the contrasting feeding strategies and P recycling observed for *B. gibbosa* and *D. chilense* differentially shape the abundance and nutritional quality of lower trophic planktonic levels (Figure 8). Prey biomass under the indirect presence of *B. gibbosa* (Figure 8a) increased significantly for CPcy, while P quota increased significantly for CPcy and micro-algae. Similarly, the indirect presence of *D. chilense* (Figure 8c) did not induce changes in prey biomass and P quota. The direct presence of *B. gibbosa* (Figure 8b) increased the P quota of all prey compartments, especially for nanoflagellates, but reduced the biomass of nanoflagellates and micro-algae. Also, the direct presence of *D. chilense* (Figure 8d) sharply reduced biomass of heterotrophic bacteria and single-cell Pcy, increased CPcy biomass, but did not change the biomass of nanoflagellates and micro-algae. In addition, the direct presence of *D. chilense* (Figure 8d) sharply increased the P quota of heterotrophic bacteria, Pcy, CPcy and micro-algae but reduced the P quota of nanoflagellates.

4 | DISCUSSION

The outcomes of predator–prey interactions respond to multiple direct and indirect effects, such as consumption of prey and nutrient supply for them through excretion (Branco et al., 2018; Schmitz et al., 2010). Here, we present a model that generalises the effect of zooplankton on lower trophic levels with contrasting strategies in terms of grazing and P recycling. Our Bayesian modelling approach allowed us to estimate these variables based on our experimental results and prior information of P utilisation traits (Edwards et al., 2012) and growth rate of the microbial compartments and phytoplankton (Tambi et al., 2009). Moreover, from the observed dynamics of prey biomass and dissolved and particulate P concentration, we were able

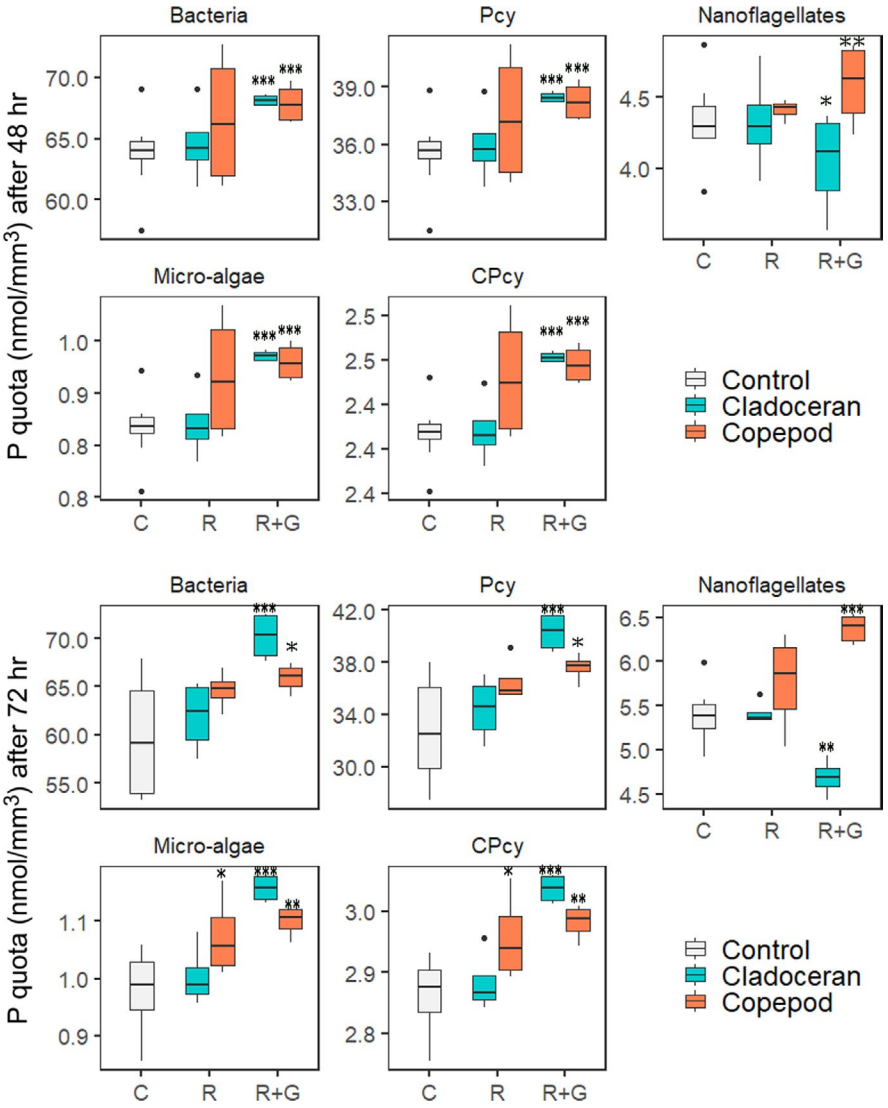

FIGURE 6 Model-estimated prey P quota after 48- and 72-hr incubation of the five prey compartments under the direct and indirect presence of the cladoceran *Diaphanosoma chilense* and the copepod *Boeckella gibbosa*. C = control treatments with no zooplankton (R and R + G pooled together); R = recycling treatments with zooplankton and prey separated by dialysis bags; R + G = grazing treatment with direct contact between zooplankton and prey. Black dots correspond to outliers and black asterisks represent differences between the posterior probability distributions of the zooplankton treatments and the control where more than 75% has the same sign as the mean posterior difference (* > 99%, ** > 90%, *** > 75%)

to estimate the non-observed dynamics of prey P quota and predict zooplankton P acquisition and excretion rates.

Our model was able to predict zooplankton P acquisition and excretion rates based on the results of our field experiment and body C:P ratios. P excretion rate was higher for the copepod *B. gibbosa* than the cladoceran *D. chilense*, as expected from the ecological stoichiometry theory and empirical evidence (Hébert et al., 2017; Sterner & Elser, 2002). Although we did not provide prior information on different P excretion rates for these zooplankton, our model results showed similar values to those independently obtained in the laboratory experiments. Therefore, we showed that indirect predator–prey interactions, which are usually difficult to measure in the field, such as nutrient excretion rates, can be assessed by modelling more conspicuous variables, such as prey biomass, nutrient concentration, and zooplankton C:P ratios. Moreover, according to our model, grazing on different prey results in a higher P acquisition for cladocerans than copepods, despite P release being higher in the latter. For the copepod *B. gibbosa*, P acquisition is given by grazing on nanoflagellates and larger phytoplankton species such as diatoms and dinoflagellates, which have lower P quotas than small cells. On the contrary, P acquisition for the cladoceran *D. chilense* was given by high grazing rates on P-rich picoplankton rather than larger cells.

The contrasting feeding strategies of copepods and cladocerans differentially shape the microbial community and the interactions within it (Vrede & Vrede, 2005; Zöllner et al., 2003). According to our expectations, we found experimentally that direct presence of the copepod *B. gibbosa* reduced the biomass of the large prey compartments (nanoflagellates and micro-algae) while the cladoceran *D. chilense* reduced the biomass of the small compartments (heterotrophic bacteria and Pcy). Grazing on different prey sizes probably allows two planktonic species to co-occur (Sommer & Stibor, 2002). Bacterial production is linked to copepods through protists (Sommer & Sommer, 2006), and this was the case for *B. gibbosa*, which showed high grazing rates on bacterivorous nanoflagellates. However, the high grazing efficiency of *D. chilense* on picoplankton represents a shortcut for their high P requirement in an oligotrophic P-limited lake. In addition, the position of *D. chilense* as an omnivore would increase the connectance and stability of the food web (Kratina et al., 2012) particularly in low productivity systems (France, 2012). Moreover, our results and the outputs of our model imply that the

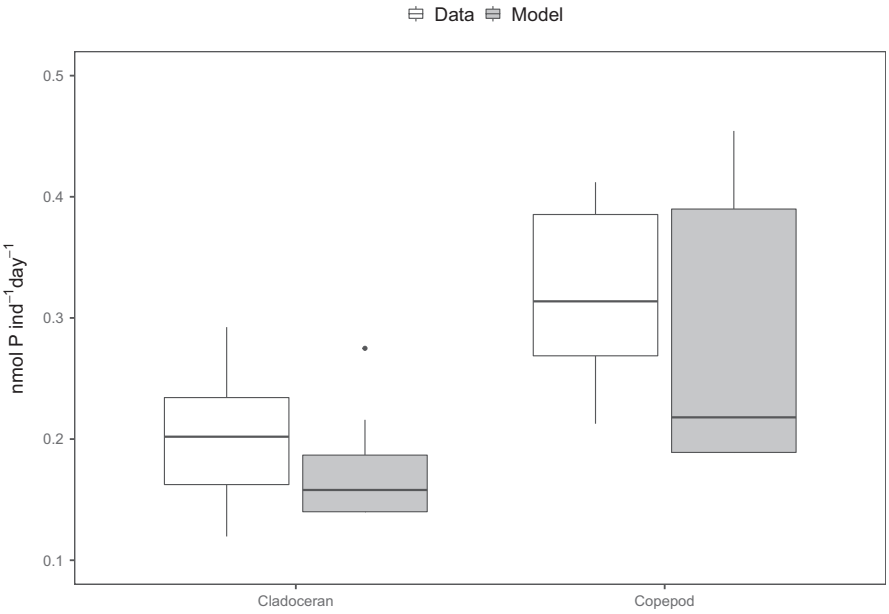

FIGURE 7 Phosphorus recycling rates of the cladoceran *Diaphanosoma chilense* and the copepod *Boeckella gibbosa* obtained in the excretion experiments (white boxes) and estimated by the model (grey boxes)

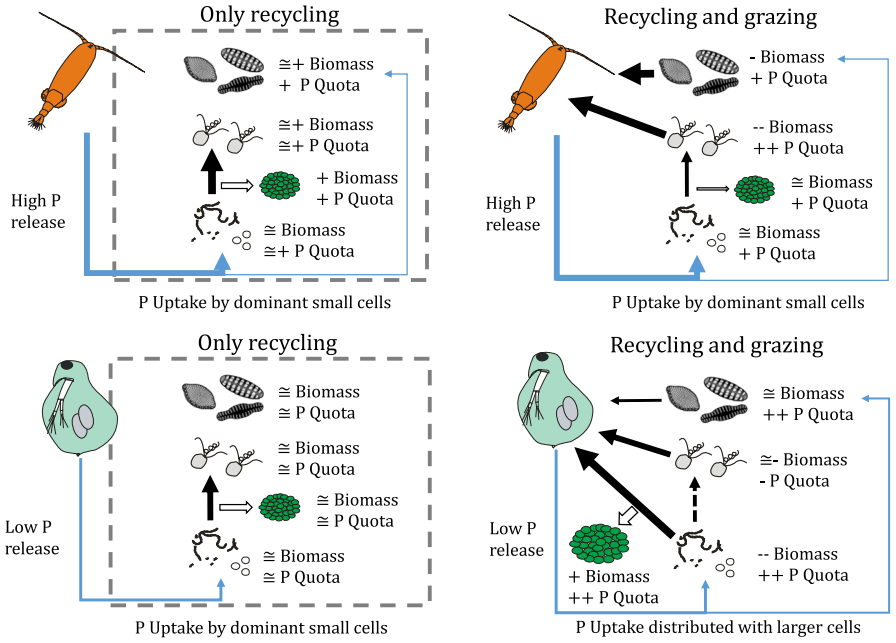

FIGURE 8 Conceptual synthesis of the direct and indirect effects of the copepod *Boeckella gibbosa* and the cladoceran *Diaphanosoma chilense* on the different microbial compartments through grazing and nutrient recycling. The arrows size suggests the strength of the interaction according to our experimental results and model predictions. Black arrows represent grazing, white arrows represent picoplanktonic cyanobacteria aggregation in colonies. The symbols accompanying biomass and P quota indicate differences from the control (no zooplankton treatments): ≅ no appreciable changes; ≅+ increasing trend; + significant increase; ++ high increase; ≅- decreasing trend; - significant decrease; -- high decrease

strong negative effect of *D. chilense* on mixotrophic nanoflagellates is through competition for picoplanktonic prey rather than direct grazing.

Bacterivorous protists are considered a key link between bacterial production and higher consumers (Gaedke et al., 2002; Yvon-Durocher et al., 2017). We found that the main P uptake in nanoflagellates is through bacterivory. Accordingly, P quota of nanoflagellates followed a different path than the other osmotrophic compartments considered in our model. This situation is expected since this group was dominated by highly bacterivorous mixotrophic species (i.e. *C. parva*). The highest P quota of nanoflagellates was found under the direct presence of *B. gibbosa*, where picoplankton biomass increased due to a high P recycling with a concomitant decrease in nanoflagellate biomass due to grazing. On the contrary, the lowest P quota of nanoflagellates was found in the direct presence of *D. chilense*, which reduced picoplankton biomass, therefore

limiting the main P source for nanoflagellates. These results place mixotrophic nanoflagellates, in terms of their P quota, as a highly sensitive compartment, affected by differential zooplankton grazing and nutrient recycling. Current models of planktonic food webs identify mixotrophy as a key interaction affected by environmental variables such as light, turbidity, and dissolved nutrients (Fischer et al., 2017; Schenone et al., 2020). As light decreases and nutrients increase, an increase in osmotrophy over phagotrophy in mixotrophic protists was predicted by mechanistic models (Berge et al., 2017; Mitra et al., 2016) as well as experimental and field observations (Fischer et al., 2017; Ptacnik et al., 2004; Waibel et al., 2019). In this continuum of feeding strategies, the relative importance of phagotrophy over osmotrophy in P uptake will also vary. Thus, our result that nanoflagellate bacterivory P uptake exceeds osmotrophy is not generalisable. However, our model allows us to disentangle and distinguish between these two pathways in P uptake.

The ability to store internal P is a key trait within the planktonic microbial loop and phytoplankton in P-limited systems (Edwards et al., 2012; Tambi et al., 2009). The model-estimated P quota for the strictly osmotrophic prey compartments (heterotrophic bacteria, Pcy, CPcy, and micro-algae) increased in all zooplankton treatments except for the indirect presence of *D. chilense*. According to this, prey P quota increases with direct presence of both copepods and cladocerans, however, the underlying mechanisms are different. Predators can increase the nutrient quality of the overall prey community by increasing the availability of the limiting nutrient, but also by grazing upon the best competitors for this nutrient (Sterner & Elser, 2002; Vrede & Vrede, 2005). *Boeckella gibbosa* increased prey P quota indirectly by releasing more P to the environment and thus both direct and indirect presence had similar effects. *D. chilense* increased prey P quota only directly by grazing on picoplankton, the best competitors for P (Tambi et al., 2009). Such findings suggest that, despite being considered as a P sink due to their higher requirement for this element (Elser & Urabe, 1999), highly bacterivorous cladocerans can mediate the P flux between bacteria and phytoplankton in P-limited systems (Pomati et al., 2020).

Finally, we also found an increase of CPcy biomass with the direct presence of *D. chilense* and under nanoflagellate bacterivory. Aggregation is a strategy for small cells to escape from predation by increasing their size and thus the handling time of the predator (Boenigk & Arndt, 2002; Huber et al., 2017). Moreover, the presence of a gelatinous matrix in larger CPcy acts as an effective anti-grazing agent (Callieri, 2010). However, P affinity decreases with size (Edwards et al., 2012) thus aggregation would imply a trade-off between grazing avoidance and acquisition of essential nutrients. The high grazing pressure exerted by the cladoceran *D. chilense*, which can access bigger particles than nanoflagellates, triggered larger colony sizes. Accordingly, model-estimated biomass increments by aggregation were higher than intrinsic growth and higher for *D. chilense* than for nanoflagellates. In addition, the slight decrease in CPcy biomass and number of cells per colony found under the direct presence of the copepod *B. gibbosa* was probably more related to a top-down control on nanoflagellates than direct grazing. Together with an observed increase of Pcy and heterotrophic bacteria in this treatment, these results support the idea that top-down control by copepods on bacterivorous protozoans favours the small and single-cell picoplankton (Callieri, 2010; Vrede & Vrede, 2005).

Currently, there is a gradient in planktonic food web models from more conceptual (Branco et al., 2020; Loladze et al., 2000) to experimental models (Gaedke et al., 2002; Rogers et al., 2020). Consequently, modelling approaches combining mechanistic models with accurate experiments within a proper statistical framework are arising (Lignell et al., 2013; Rosenbaum et al., 2019). In this work, we studied how the microbial community is structured in the short term by two important members of the zooplankton. Copepods and cladocerans constitute the dominant zooplankton groups in lakes and their dominance fluctuates seasonally, depending on conditions such as temperature, turbidity, and nutrient concentration (Gliwicz & Pijanowska, 1989; Laspoumaderes et al., 2013; Schaffner et al., 2019). According to our model results, copepods would favour higher P acquisition rates for cladocerans by releasing more P for picoplankton. By contrast, cladocerans would have a mixed effect on the main food items of copepods by increasing P quotas of the strictly osmotrophic algae but decreasing P quotas of mixotrophic nanoflagellates. The model presented here could be used to disentangle complex pathways in the microbial food web. In this sense, the relative importance of phagotrophy and osmotrophy in P uptake, P quotas and nutrient recycling by grazers are important variables that can be assessed quantitatively with our model. These are key variables for understanding ecosystem matter flux and resource use efficiency.

ACKNOWLEDGMENTS

L.S. is a CONICET fellowship, all other authors are CONICET researchers, and C.L. was supported by the Alexander von Humboldt Foundation. This work was supported by the Fondo Para la Investigación Científica y Tecnológica Argentina (FONCyT), PICT 2017-1940, PICT 2018-1563, CONICET PUE2016-0008. Sampling and experiments were conducted with permission N°734 by Administración Parques Nacionales, Argentina.

CONFLICT OF INTEREST

The authors declare no competing interests.

AUTHOR CONTRIBUTIONS

L.S., E.B., and B.M. conceived the study, designed experiments, analysed data and wrote the manuscript. L.S. carried out the experiments and laboratory determination and developed the model. N.M., M.B.N., and C.L. carried out experiments and laboratory determinations. All authors contributed to the final manuscript.

DATA AVAILABILITY STATEMENT

All the data generated during and/or analysed during the current study will be available at the Universidad Nacional del Comahue data repository http://rdi.uncoma.edu.ar//handle/123456789/16092

ORCID

Luca Schenone https://orcid.org/0000-0003-3025-7133
Beatriz Modenutti https://orcid.org/0000-0002-8683-5679
Nicolás Martyniuk https://orcid.org/0000-0002-2423-7040
Marcela Bastidas Navarro https://orcid.org/0000-0002-6558-0451
Cecilia Laspoumaderes https://orcid.org/0000-0001-7790-2975
Esteban Balseiro https://orcid.org/0000-0002-5052-0587

REFERENCES

Anderson, T. R. (2005). Plankton functional type modelling: Running before we can walk? *Journal of Plankton Research*, *27*, 1073–1081. https://doi.org/10.1093/plankt/fbi076

APHA. (2005). *Standard methods for the examination of water and wastewater*. American Public Health Association, AWWA.

Arhonditsis, G. B., Papantou, D., Zhang, W., Perhar, G., Massos, E., & Shi, M. (2008). Bayesian calibration of mechanistic aquatic biogeochemical models and benefits for environmental management. *Journal of Marine Systems*, *73*, 8–30. https://doi.org/10.1016/j.jmarsys.2007.07.004

Atkinson, C. L., Capps, K. A., Rugenski, A. T., & Vanni, M. J. (2017). Consumer-driven nutrient dynamics in freshwater ecosystems: From individuals to ecosystems. *Biological Reviews*, *92*, 2003–2023. https://doi.org/10.1111/brv.12318

Attayde, J. L., & Hansson, L.-A. (1999). Effects of nutrient recycling by zooplankton and fish on phytoplankton communities. *Oecologia*, *121*, 47–54. https://doi.org/10.1007/s004420050906

Azam, F., Fenchel, T., Field, J. G., Gray, J., Meyer-Reil, L., & Thingstad, F. (1983). The ecological role of water-column microbes in the sea. *Marine Ecology Progress Series*, *10*, 257–263. https://doi.org/10.3354/meps010257

Balseiro, E. G., Modenutti, B. E., & Queimalffiños, C. P. (1997). Nutrient recycling and shifts in N:P ratio by different zooplankton structures in a South Andes lake. *Journal of Plankton Research*, *19*, 805–817. https://doi.org/10.1093/plankt/19.7.805

Balseiro, E. G., Modenutti, B. E., & Queimaliños, C. P. (2001). Feeding of *Boeckella gracilipes* (Copepoda, Calanoida) on ciliates and phytoflagellates in an ultraoligotrophic Andean lake. *Journal of Plankton Research*, *23*, 849–857. https://doi.org/10.1093/plankt/23.8.849

Berge, T., Chakraborty, S., Hansen, P. J., & Andersen, K. H. (2017). Modeling succession of key resource-harvesting traits of mixotrophic plankton. *The ISME Journal*, *11*, 212–223. https://doi.org/10.1038/ismej.2016.92

Boenigk, J., & Arndt, H. (2002). Bacterivory by heterotrophic flagellates: Community structure and feeding strategies. *Antonie Van Leeuwenhoek*, *81*, 465–480.

Branco, P., Egas, M., Elser, J. J., & Huisman, J. (2018). Eco-evolutionary dynamics of ecological stoichiometry in plankton communities. *The American Naturalist*, *192*, E1–E20. https://doi.org/10.1086/697472

Branco, P., Egas, M., Hall, S. R., & Huisman, J. (2020). Why do phytoplankton evolve large size in response to grazing? *The American Naturalist*, *195*, E20–E37. https://doi.org/10.1086/706251

Brendelberger, H. (1991). Filter mesh size of cladocerans predicts retention efficiency for bacteria. *Limnology and Oceanography*, *36*, 884–894. https://doi.org/10.4319/lo.1991.36.5.0884

Burns, C. W., & Schallenberg, M. (1996). Relative impacts of copepods, cladocerans and nutrients on the microbial food web of a mesotrophic lake. *Journal of Plankton Research*, *18*, 683–714. https://doi.org/10.1093/plankt/18.5.683

Callieri, C. (2010). Single cells and microcolonies of freshwater picocyanobacteria: A common ecology. *Journal of Limnology*, *69*, 257. https://doi.org/10.4081/jlimnol.2010.257

Carrillo, P., Medina-Sánchez, J., Villar-Argaiz, M., Bullejos, F., Durán, C., Bastidas-Navarro, M., … Modenutti, B. E. (2017). Vulnerability of mixotrophic algae to nutrient pulses and UVR in an oligotrophic Southern and Northern Hemisphere lake. *Scientific Reports*, *7*, 1–11. https://doi.org/10.1038/s41598-017-06279-9

Clark, J. S. (2005). Why environmental scientists are becoming Bayesians. *Ecology Letters*, *8*, 2–14. https://doi.org/10.1111/j.1461-0248.2004.00702.x

Cotner, J. B., & Biddanda, B. A. (2002). Small players, large role: Microbial influence on biogeochemical processes in pelagic aquatic ecosystems. *Ecosystems*, *5*, 105–121. https://doi.org/10.1007/s10021-001-0059-3

Droop, M. R. (1968). Vitamin B12 and marine ecology. IV. The kinetics of uptake, growth and inhibition in *Monochrysis lutheri*. *Journal of the Marine Biological Association of the United Kingdom*, *48*, 689–733.

Droop, M. R. (1973). Some thoughts on nutrient limitation in algae 1. *Journal of Phycology*, *9*, 264–272.

Edwards, K. F., Thomas, M. K., Klausmeier, C. A., & Litchman, E. (2012). Allometric scaling and taxonomic variation in nutrient utilization traits and maximum growth rate of phytoplankton. *Limnology and Oceanography*, *57*, 554–566. https://doi.org/10.4319/lo.2012.57.2.0554

Elser, J. J., Dobberfuhl, D. R., MacKay, N. A., & Schampel, J. H. (1996). Organism size, life history, and N:P stoichiometry: Toward a unified view of cellular and ecosystem processes. *BioScience*, *46*, 674–684. https://doi.org/10.2307/1312897

Elser, J. J., Elser, M. M., MacKay, N. A., & Carpenter, S. R. (1988). Zooplankton-mediated transitions between N-and P-limited algal growth 1. *Limnology and Oceanography*, *33*, 1–14. https://doi.org/10.4319/lo.1988.33.1.0001

Elser, J. J., & Urabe, J. (1999). The stoichiometry of consumer-driven nutrient recycling: Theory, observations, and consequences. *Ecology*, *80*, 735–751.

Fischer, R., Giebel, H. A., Hillebrand, H., & Ptacnik, R. (2017). Importance of mixotrophic bacterivory can be predicted by light and loss rates. *Oikos*, *126*, 713–722. https://doi.org/10.1111/oik.03539

France, R. L. (2012). Omnivory, vertical food-web structure and system productivity: Stable isotope analysis of freshwater planktonic food webs. *Freshwater Biology*, *57*, 787–794. https://doi.org/10.1111/j.1365-2427.2012.02744.x

Gaedke, U., Hochstädter, S., & Straile, D. (2002). Interplay between energy limitation and nutritional deficiency: Empirical data and food web models. *Ecological Monographs*, *72*, 251–270.

Gliwicz, Z. M., & Pijanowska, J. (1989). The role of predation in zooplankton succession. In U. Sommer(Eds.), *Plankton ecology: succession in plankton communities* (pp. 253–296). Springer.

Gophen, M., & Geller, W. (1984). Filter mesh size and food particle uptake by *Daphnia*. *Oecologia*, *64*, 408–412. https://doi.org/10.1007/BF00379140

Grover, J. P. (2004). Predation, competition, and nutrient recycling: A stoichiometric approach with multiple nutrients. *Journal of Theoretical Biology*, *229*, 31–43. https://doi.org/10.1016/j.jtbi.2004.03.001

Haario, H., Laine, M., Mira, A., & Saksman, E. (2006). DRAM: Efficient adaptive MCMC. *Statistics and Computing*, *16*, 339–354. https://doi.org/10.1007/s11222-006-9438-0

Hébert, M.-P., Beisner, B. E., & Maranger, R. (2017). Linking zooplankton communities to ecosystem functioning: Toward an effect-trait framework. *Journal of Plankton Research*, *39*, 3–12. https://doi.org/10.1093/plankt/fbw068

Hessen, D., Andersen, T., & Faafeng, B. (1992). Zooplankton contribution to particulate phosphorus and nitrogen in lakes. *Journal of Plankton Research*, *14*, 937–947. https://doi.org/10.1093/plankt/14.7.9376

Holling, C. S. (1959). Some characteristics of simple types of predation and parasitism. *Canadian Entomologist*, *91*, 385–398. https://doi.org/10.4039/Ent91385-7

Huber, P., Diovisalvi, N., Ferraro, M., Metz, S., Lagomarsino, L., Llames, M. E., Royo-Llonch, M., … Acinas, S. G. (2017). Phenotypic plasticity in freshwater picocyanobacteria. *Environmental Microbiology*, *19*, 1120–1133.

Jürgens, K. (1994). Impact of *Daphnia* on planktonic microbial food webs—A review. *Marine Microbial Food Webs*, *8*, 295–324.

Kemp, P. F., Cole, J. J., Sherr, B. F., & Sherr, E. B. (1993). *Handbook of methods in aquatic microbial ecology*. CRC Press.

Kratina, P., LeCraw, R. M., Ingram, T., & Anholt, B. R. (2012). Stability and persistence of food webs with omnivory: Is there a general pattern? *Ecosphere*, *3*, 1–18. https://doi.org/10.1890/ES12-00121.1

Laspoumaderes, C., Modenutti, B., Elser, J. J., & Balseiro, E. (2015). Does the stoichiometric carbon: Phosphorus knife edge apply for predaceous copepods? *Oecologia*, *178*, 557–569. https://doi.org/10.1007/s00442-014-3155-8

Laspoumaderes, C., Modenutti, B. E., Souza, M. S., Bastidas Navarro, M., Cuassolo, F., & Balseiro, E. G. (2013). Glacier melting and stoichiometric implications for lake community structure: Zooplankton species distributions across a natural light gradient. *Global Change Biology*, *19*, 316–326. https://doi.org/10.1111/gcb.12040

Li, Y., Gal, G., Makler-Pick, V., Waite, A., Bruce, L., & Hipsey, M. (2014). Examination of the role of the microbial loop in regulating lake nutrient stoichiometry and phytoplankton dynamics. *Biogeosciences*, *11*, 2939–2960. https://doi.org/10.5194/bg-11-2939-2014

Lignell, R., Haario, H., Laine, M., & Thingstad, T. F. (2013). Getting the "right" parameter values for models of the pelagic microbial food web. *Limnology and Oceanography*, *58*, 301–313. https://doi.org/10.4319/lo.2013.58.1.0301

Loladze, I., Kuang, Y., & Elser, J. J. (2000). Stoichiometry in producer-grazer systems: Linking energy flow with element cycling. *Bulletin of Mathematical Biology*, *62*, 1137–1162. https://doi.org/10.1006/bulm.2000.0201

Loreau, M., & De Mazancourt, C. (2013). Biodiversity and ecosystem stability: A synthesis of underlying mechanisms. *Ecology Letters*, *16*, 106–115. https://doi.org/10.1111/ele.12073

Malve, O., Laine, M., Haario, H., Kirkkala, T., & Sarvala, J. (2007). Bayesian modelling of algal mass occurrences—Using adaptive MCMC methods with a lake water quality model. *Environmental Modelling & Software*, *22*, 966–977. https://doi.org/10.1016/j.envsoft.2006.06.016

Markert, B., Pedrozo, F., Geller, W., Friese, K., Korhammer, S., Baffico, G., Diaz, M., & Wolfl, S. (1997). A contribution to the study of the heavy-metal and nutritional element status of some lakes in the southern Andes of Patagonia (Argentina). *Science of the Total Environment*, *206*, 1–15. https://doi.org/10.1016/S0048-9697(97)00218-0

Mitra, A., Flynn, K. J., Tillmann, U., Raven, J. A., Caron, D., Stoecker, D. K., … Lundgren, V. (2016). Defining planktonic protist functional groups on mechanisms for energy and nutrient acquisition: Incorporation of diverse mixotrophic strategies. *Protist*, *167*, 106–120. https://doi.org/10.1016/j.protis.2016.01.003

Modenutti, B. E., Queimaliños, C. P., Balseiro, E. G., & Reissig, M. (2003). Impact of different zooplankton structures on the microbial food web of a South Andean oligotrophic lake. *Acta Oecologica*, *24*, S289–S298. https://doi.org/10.1016/S1146-609X(03)00030-4

Plummer, M. (2003). JAGS: A program for analysis of Bayesian graphical models using Gibbs sampling. In *Proceedings of the 3rd international workshop on distributed statistical computing*, vol. *124*, p. 10.

Pomati, F., Shurin, J. B., Andersen, K. H., Tellenbach, C., & Barton, A. D. (2020). Interacting temperature, nutrients and zooplankton grazing control phytoplankton size-abundance relationships in eight Swiss lakes. *Frontiers in Microbiology*, *10*, 3155. https://doi.org/10.3389/fmicb.2019.03155

Porter, K. G., & Feig, Y. S. (1980). The use of DAPI for identifying and counting aquatic microflora 1. *Limnology and Oceanography*, *25*, 943–948. https://doi.org/10.4319/lo.1980.25.5.0943

Ptacnik, R., Sommer, U., Hansen, T., & Martens, V. (2004). Effects of microzooplankton and mixotrophy in an experimental planktonic food web. *Limnology and Oceanography*, *49*, 1435–1445. https://doi.org/10.4319/lo.2004.49.4_part_2.1435

R Team. (2020). *RStudio: Integrated development for R*. RStudio Inc.

Rogers, T. L., Munch, S. B., Stewart, S. D., Palkovacs, E. P., Giron-Nava, A., Matsuzaki, S.-I., & Symons, C. C. (2020). Trophic control changes with season and nutrient loading in lakes. *Ecology Letters*, *23*, 1287–1297. https://doi.org/10.1111/ele.13532

Rosenbaum, B., Raatz, M., Weithoff, G., Fussmann, G. F., & Gaedke, U. (2019). Estimating parameters from multiple time series of population dynamics using Bayesian inference. *Frontiers in Ecology and Evolution*, *6*, 234. https://doi.org/10.3389/fevo.2018.00234

Sanders, R. W., Porter, K. G., Bennett, S. J., & DeBiase, A. E. (1989). Seasonal patterns of bacterivory by flagellates, ciliates, rotifers, and cladocerans in a freshwater planktonic community. *Limnology and Oceanography*, *34*, 673–687. https://doi.org/10.4319/lo.1989.34.4.0673

Schaffner, L. R., Govaert, L., De Meester, L., Ellner, S. P., Fairchild, E., Miner, B. E., … Hairston, N. G. (2019). Consumer-resource dynamics is an eco-evolutionary process in a natural plankton community. *Nature Ecology and Evolution*, *3*, 1351–1358. https://doi.org/10.1038/s41559-019-0960-9

Schenone, L., Balseiro, E. G., Bastidas Navarro, M., & Modenutti, B. E. (2020). Modelling the consequence of glacier retreat on mixotrophic nanoflagellate bacterivory: A Bayesian approach. *Oikos*, *129*, 1216–1228. https://doi.org/10.1111/oik.07170

Schmitz, O. J., Hawlena, D., & Trussell, G. C. (2010). Predator control of ecosystem nutrient dynamics. *Ecology Letters*, *13*, 1199–1209. https://doi.org/10.1111/j.1461-0248.2010.01511.x

Sherr, B. F., Sherr, E. B., & Fallon, R. D. (1987). Use of monodispersed, fluorescently labeled bacteria to estimate in situ protozoan bacterivory. *Applied and Environment Microbiology*, *53*, 958–965.

Sherr, E.B., & Sherr, B.F. (1993). Protistan grazing rates via uptake of fluorescently labeled prey. In P.F. Kemp, J.J. Cole, B.F. Sherr & E.B. Sherr(Eds.), *Handbook of methods in aquatic microbial ecology*.(pp. 695–701). Lewis Publisher.

Šimek, K., & Chrzanowski, T. H. (1992). Direct and indirect evidence of size-selective grazing on pelagic bacteria by freshwater nanoflagellates. *Applied and Environment Microbiology*, *58*, 3715–3720.

Sitters, J., Bakker, E. S., Veldhuis, M. P., Veen, G., Olde Venterink, H., & Vanni, M. J. (2017). The stoichiometry of nutrient release by terrestrial herbivores and its ecosystem consequences. *Frontiers in Earth Science*, *5*, 32. https://doi.org/10.3389/feart.2017.00032

Sommer, U., & Sommer, F. (2006). Cladocerans versus copepods: The cause of contrasting top–down controls on freshwater and marine phytoplankton. *Oecologia*, *147*, 183–194. https://doi.org/10.1007/s00442-005-0320-0

Sommer, U., & Stibor, H. (2002). Copepoda–Cladocera–Tunicata: The role of three major mesozooplankton groups in pelagic food webs. *Ecological Research*, *17*, 161–174. https://doi.org/10.1046/j.1440-1703.2002.00476.x

Souza, M., Modenutti, B., Carrillo, P., Villar-Argaiz, M., Medina-Sánchez, J., Bullejos, F., & Balseiro, E. (2010). Stoichiometric dietary constraints influence the response of copepods to ultraviolet radiation-induced oxidative stress. *Limnology and Oceanography*, *55*, 1024–1032. https://doi.org/10.4319/lo.2010.55.3.1024

Sterner, R. W., & Elser, J. J. (2002). *Ecological stoichiometry: The biology of elements from molecules to the biosphere*. Princeton University Press.

Sun, J., & Liu, D. (2003). Geometric models for calculating cell biovolume and surface area for phytoplankton. *Journal of Plankton Research*, *25*, 1331–1346. https://doi.org/10.1093/plankt/fbg096

Tambi, H., Flaten, G. A. F., Egge, J. K., Bødtker, G., Jacobsen, A., & Thingstad, T. F. (2009). Relationship between phosphate affinities and cell size and shape in various bacteria and phytoplankton.

Aquatic Microbial Ecology, *57*, 311–320. https://doi.org/10.3354/ame01369

Vanni, M. J. (2002). Nutrient cycling by animals in freshwater ecosystems. *Annual Review of Ecology and Systematics*, *33*, 341–370. https://doi.org/10.1146/annurev.ecolsys.33.010802.150519

Villar-Argaiz, M., Balseiro, E.G., Modenutti, B.E., Souza, M.S., Bullejos, F.J., Medina-Sánchez, J.M, & Carrillo, P. (2018). Resource versus consumer regulation of phytoplankton: Testing the role of UVR in a Southern and Northern hemisphere lake. *Hydrobiologia*, *816*, 107–120.

Vrede, T., & Vrede, K. (2005). Contrasting 'top-down' effects of crustacean zooplankton grazing on bacteria and phytoflagellates. *Aquatic Ecology*, *39*, 283–293. https://doi.org/10.1007/s10452-005-1326-8

Waibel, A., Peter, H., & Sommaruga, R. (2019). Importance of mixotrophic flagellates during the ice-free season in lakes located along an elevational gradient. *Aquatic Sciences*, *81*, 45. https://doi.org/10.1007/s00027-019-0643-2

Yvon-Durocher, G., Schaum, C.-E., & Trimmer, M. (2017). The temperature dependence of phytoplankton stoichiometry: Investigating the roles of species sorting and local adaptation. *Frontiers in Microbiology*, *8*, 2003. https://doi.org/10.3389/fmicb.2017.02003

Zhang, W., & Arhonditsis, G. B. (2009). A Bayesian hierarchical framework for calibrating aquatic biogeochemical models. *Ecological Modelling*, *220*, 2142–2161. https://doi.org/10.1016/j.ecolmodel.2009.05.023

Zöllner, E., Santer, B., Boersma, M., Hoppe, H. G., & Jürgens, K. (2003). Cascading predation effects of *Daphnia* and copepods on microbial food web components. *Freshwater Biology*, *48*, 2174–2193.

SUPPORTING INFORMATION

Additional supporting information may be found in the online version of the article at the publisher's website.

How to cite this article: Schenone, L., Modenutti, B., Martyniuk, N., Bastidas Navarro, M., Laspoumaderes, C., & Balseiro, E. (2021). Modelling key variables for understanding the effects of grazing and nutrient recycling by zooplankton on the freshwater microbial loop. *Freshw Biol.*, 66, 2322–2337. https://doi.org/10.1111/fwb.13835